

Reprogramming of human fibroblasts into osteoblasts by insulin-like growth factor-binding protein 7

ZuFu Lu^{1,2}  | Joyce Chiu³ | Lucinda R. Lee^{4,5} | Aaron Schindeler^{4,5} | Miriam Jackson¹ | Yogambha Ramaswamy^{1,2} | Colin R. Dunstan^{1,2} | Philip J. Hogg³ | Hala Zreiqat^{1,2}

¹Tissue Engineering & Biomaterials Research Unit, School of Biomedical Engineering, The University of Sydney, Camperdown, New South Wales, Australia

²ARC Training Centre for Innovative BioEngineering, The University of Sydney, Camperdown, New South Wales, Australia

³The Centenary Institute, NHMRC Clinical Trial Centre, The University of Sydney, Camperdown, New South Wales, Australia

⁴Bioengineering & Molecular Medicine, The Children's Hospital at Westmead, Westmead, New South Wales, Australia

⁵Discipline of Child and Adolescent Medicine, The University of Sydney, Camperdown, New South Wales, Australia

Correspondence

Zufu Lu, PhD, MD, and Hala Zreiqat, PhD, Biomaterials and Tissue Engineering Research Unit, School of Biomedical Engineering, the University of Sydney, Camperdown, NSW, 2006, Australia.

Email: zufu.lu@sydney.edu.au (Z. L.), hala.zreiqat@sydney.edu.au (H. Z.)

Funding information

National Health and Medical Research Council of Australia, Grant/Award Numbers: APP1139515, APP1110219; Australian Research Council; University of Sydney Bridging Fellowship; National Health and Medical Research Council (NHMRC) Early Career Fellowships, Grant/Award Number: APP1036370

Abstract

The induced pluripotent stem cell (iPSC) is a promising cell source for tissue regeneration. However, the therapeutic value of iPSC technology is limited due to the complexity of induction protocols and potential risks of teratoma formation. A trans-differentiation approach employing natural factors may allow better control over reprogramming and improved safety. We report here a novel approach to drive trans-differentiation of human fibroblasts into functional osteoblasts using insulin-like growth factor binding protein 7 (IGFBP7). We initially determined that media conditioned by human osteoblasts can induce reprogramming of human fibroblasts to functional osteoblasts. Proteomic analysis identified IGFBP7 as being significantly elevated in media conditioned with osteoblasts compared with those with fibroblasts. Recombinant IGFBP7 induced a phenotypic switch from fibroblasts to osteoblasts. The switch was associated with senescence and dependent on autocrine IL-6 signaling. Our study supports a novel strategy for regenerating bone by using IGFBP7 to trans-differentiate fibroblasts to osteoblasts.

KEYWORDS

human fibroblast, IGFBP7, IL-6, osteoblast, reprogramming, senescence

1 | INTRODUCTION

Human tissues such as the skin, blood, and bone are capable of self-repairing and regeneration. Large bone defects and loss due to cancer or trauma can lead to scar tissue formation that impairs the bones ability to

repair and regenerate. The current “gold standard” treatment, autografts, has its inherent drawbacks, including limited availability and donor site morbidity, and an alternative source of bone cells is thus required. The success of induced pluripotent stem cell (iPSC) technology to reprogram fibroblasts to progenitor cells of various lineages offers an exciting route for tissue

This is an open access article under the terms of the Creative Commons Attribution-NonCommercial License, which permits use, distribution and reproduction in any medium, provided the original work is properly cited and is not used for commercial purposes.

© 2020 The Authors. STEM CELLS TRANSLATIONAL MEDICINE published by Wiley Periodicals, Inc. on behalf of AlphaMed Press

repair and regeneration. iPSC technology represents a potentially unlimited source of progenitor cells for therapeutic applications. It also allows patients to use their own cells for tissue repair and regeneration and thus poses little or no risk of immune rejection that can be associated with allogeneic bone transplants. Nonetheless, the prospect of using iPSC technology for tissue regeneration is more challenging than initially anticipated since terminally differentiated cells require complex reprogramming using the Yamanaka factors (Oct3/4, Sox2, Klf4, c-Myc). To add to the complexity, specific stimuli are required to direct iPSC to re-differentiate to progenitor cells of the lineage of interest. In addition, any remaining iPSC poses risk of teratoma formation following implantation.¹ These issues have limited the therapeutic value of iPSC technology in tissue regeneration.

Differentiated cells such as fibroblasts can trans-differentiate into other somatic cell types through reprogramming, thus overcome the limitations of using iPSCs. Recent studies have demonstrated direct reprogramming of fibroblasts into various somatic cell types including cardiomyocytes, neurons.²⁻⁶ Most of these studies, however, relied on genetic manipulation of one or more transcription regulators, raising a myriad of technical and safety issues associated with viral transduction technology, mutagenesis, and cancer risk.⁷ A chemical approach to trans-differentiation may be more amenable to clinical translation. Chemical induction of cell reprogramming is generally rapid and reversible, and is also more amenable to control through factor dosage and/or combinations with other molecules. Chemical approaches have successfully been employed to induce differentiation of embryonic stem cells to neural progenitor cells⁸ as well as to reverse differentiate somatic cells into iPSCs.⁹⁻¹¹

In cell culture, fibroblasts are morphologically similar to osteoblasts. They have generally similar gene expression profiles but lack osteoblast-specific transcripts such as *Runx2* and *Osteocalcin*.^{12,13} Their similar transcriptomic profiles led us to hypothesize that distinct factors produced by osteoblasts may be capable of inducing trans-differentiation of fibroblasts into osteoblast-like cells (OB). In this study, we sought to identify factors in media conditioned with human OB that are capable of reprogramming fibroblasts into osteoblasts. We found that insulin-like growth factor binding protein-7 (IGFBP7) is significantly elevated in media conditioned by osteoblasts compared to that by fibroblasts. Exogenous addition of recombinant IGFBP7 to growth media was sufficient to switch the phenotype from fibroblasts to osteoblasts *in vitro*. IGFBP7 treated fibroblasts produced mineralized tissue in a mouse xenograft model of ectopic bone formation. Induction of a senescent phenotype and autocrine IL-6 signaling in fibroblasts contribute to IGFBP7-mediated reprogramming. This chemical approach employing recombinant IGFBP7 for trans-differentiation of fibroblasts into osteoblasts may enable future cell-based therapies for bone tissue engineering.

2 | MATERIALS AND METHODS

2.1 | Cell culture

Permission to use discarded human tissue was granted by the Sydney Children's Hospitals Network Human Research Ethics Committee and informed consent was obtained. Human trabecular bone was used for isolating HOBs as described previously.¹⁴ The cells were cultured at 37°C

Significance statement

Bone tissue engineering is a growing field, where cell therapies have considerable translational potential. Current cell-based approaches are constrained by a limited capacity to harvest osteoblasts, mesenchymal stem cells, and a poor osteogenic potential of isolated patient fibroblasts. This study describes an innovative approach for promoting the trans-differentiation of human fibroblasts into functional osteoblasts using a single naturally bioactive protein, insulin growth factor binding protein-7 (IGFBP7). This approach will have significant advantages over other commonly used cell sources, including iPSCs and adult mesenchymal stem cells, and will potentially lead to a shift in the current paradigm of bone regenerative medicine.

with 5% CO₂, and culture medium was changed every 3 days until cells were passaged at 80% to 90% confluence. All HOBs at passage 2 used in the experiments were the cell mixtures sourced from three independent donors. Foreskin fibroblasts were kindly donated by Prof. Rebecca Mason's group at University of Sydney. Fibroblasts cells were cultured in complete media containing DMEM (Gibco, ThermoFisher Scientific, Carlsbad, CA), supplemented with 10% (v/v) fetal calf serum (FCS, ThermoFisher Scientific), 30 mg/mL penicillin, 100 mg/mL streptomycin (ThermoFisher Scientific). Cells were cultured at 37°C with 5% CO₂, and culture medium was changed every 3 days until cells were passaged at 80% to 90% confluence. All fibroblasts at passage 10 used in the experiments were the cell mixtures sourced from three independent donors.

2.2 | Preparation of conditioned media

HOBs (at passage 2) and foreskin dermal fibroblast (at passage 10) were grown with 5% CO₂ in alpha-MEM supplemented with 10% FCS and DMEM supplemented with 10% FCS, respectively. Culture medium was removed when cells were at 80%-90% confluence, followed three washes with buffered phosphate saline (PBS) and twice with serum-free DMEM. Serum-free DMEM (15 mL) was added to cells in T75 flask to be conditioned at 37°C for 48 hours. Conditioned medium was then collected (CM-OB from HOBs and CM-FB from fibroblasts). Detached cells and debris were removed from conditioned media by passing through a 0.2 µm filter and stored at -80°C until use.

2.3 | Osteoblastic reprogramming by CM or IGFBP7

Fibroblasts were seeded in 12-well plates with 100 000 cells/well and cultured in DMEM medium supplemented with 10% FCS, 30 mg/mL penicillin and 100 mg/mL streptomycin overnight. For osteoblastic reprogramming, fibroblasts were washed three times with PBS three

times followed by addition conditioned media (FB-CM or OB-CM) containing 2% FCS without or with osteogenic components: 1 mM L-ascorbic acid phosphate magnesium salt (Sigma-Aldrich, Saint Louis) and 10 mmol/L beta-glycerophosphate (Sigma-Aldrich, Saint Louis). For study of osteoblastic reprogramming by IGFBP7, cells were washed three times with PBS followed by addition of DMEM containing 2% FCS, osteogenic components and varying concentration of IGFBP7 (0, 125, 250, 500, and 1000 ng/mL) (Sigma-Aldrich, Saint Louis). Media were changed every 3 days and cells were harvested for gene expression analysis at day 4 and 14, and day 28 for Alizarin red staining.

2.4 | Sample preparation and mass spectrometry (MS)

The CM was dialyzed against 1 mM ammonium bicarbonate buffer at 4°C.¹⁵ Dialyzed medium was lyophilized and stored at -30°C until reconstitution. Lyophilized proteins were reconstituted in 0.8 mL of 25 mM ammonium bicarbonate buffer, and the pH was adjusted to 8 using 1 M Tris-HCl (pH 9.0). Proteins were denatured and reduced with a final concentration of 1% (w/v) SDS and 10 mM TCEP (pH 7.0) at 65°C for 15 minutes followed by alkylation with 55 mM iodoacetamide at room temperature for 1 hour in the dark. Proteins were precipitated with a final concentration of 10% (w/v) trichloroacetic acid overnight at 4°C followed by centrifugation at 10 000g for 10 minutes. Protein precipitate was washed three times with ice-cold 100% (v/v) acetone, air-dried and resolubilized in 70 µL with solubilization buffer containing 100 mM Tris-HCl pH 8.0, 1 mM CaCl₂ and 8 M urea. Solubilized protein was diluted 8-fold using dilution buffer containing 100 mM Tris-HCl pH 8.0, 1 mM CaCl₂. Proteins were digested with trypsin at 37°C overnight and the reaction was stopped by the addition of trifluoroacetic acid (TFA) at a final concentration of 1% (v/v). Peptides were subjected to solid phase extraction using a HLB 96-well µelution plate (Waters) as described in the manufacturer's instructions. Peptides were eluted with an elution buffer containing 0.1% TFA, 50% (v/v) acetonitrile and dried. Peptides were reconstituted in a final volume of 40 µL of 0.1% (v/v) formic acid.

The peptides were analyzed on a Thermo Fisher Scientific Ultimate 3000. One microgram of peptides was injected and resolved on a 35 cm × 75 µm C18 reverse phase analytical column with integrated emitter using a 2%-35% acetonitrile over 60 minutes with a flow rate of 250 nL/min. The peptides were ionized by electrospray ionization at +2.0 kV. Tandem mass spectrometry analysis was carried out on a Q-Exactive Plus mass spectrometer (Thermo Fisher Scientific) using CID fragmentation. The data-dependent acquisition method acquired MS/MS spectra of the top five most abundant ions at any one point during the gradient. The peptides were ionized by electrospray ionization at +2.0 kV. Tandem mass spectrometry analysis was carried out on a Q-Exactive Plus mass spectrometer using HCD fragmentation. The data-dependent acquisition method acquired MS/MS spectra of the top 20 most abundant ions at any one point during the gradient. All the chemicals used were purchased from Sigma-Aldrich, Saint Louis.

Proteomic data were analyzed using Progenesis Q1 for Proteomics software (Nonlinear Dynamics).¹⁶ MS/MS spectra were searched against the UniProt reference proteome using an external search engine Mascot (Matrix Science). Precursor mass tolerance and fragment tolerance were set at 0.6 Da and the precursor ion charge state to 2+, 3+, and 4+. Variable modifications were defined as oxidized Met and carbamidomethyl Cys with full trypsin cleavage of up to three missed cleavages. Proteins were identified and were further refined by removing proteins that scored below 20, returned with less than two hits and were non-human. Proteins was analyzed based on their Log₂(fold change) and Log₁₀(P-value). Proteins with fold-change >5 and P-value <.01 were standardized for their expression level using their calculated z-score and were subjected to hierarchical clustering analysis by web-based program Heatmapper.¹⁷ Functional annotation of proteins was analyzed by web-based GO enrichment analysis using PANTHER over-representation test.¹⁸

2.5 | Quantitative PCR (qPCR) and immunofluorescence staining

QPCR was performed as previously described.¹⁹ For immunofluorescence staining of *Runx2* expression, anti-Runx2 antibody (Abcam, ab76956, 1:100, Cambridge, MA) followed by Alexa Fluor 488 conjugated anti-mouse antibody (ThermoFisher Scientific, A28175, 1:100, Waltham MA) were used for detection. Fluorescence was analyzed using Olympus Cell Imaging System. For quantification *Runx2* positive cells in the population, fluorescent cells in a total of 150 cells were determined from 10 images acquired under ×20 magnifications at the same exposure setting from three independent experiments.

2.6 | Assessment of mineralization

Cells cultured in various conditioned media were subjected to alizarin Red staining to assess for their calcium deposition. Briefly, at 28 days post incubation with conditioned media, cells were fixed in ice cold 70% (v/v) ethanol for 1 hour at room temperature followed by rinsing two 5-minutes wash with water. One milliliter of Alizarin Red Solution (pH: 4.2, Sigma-Aldrich, Saint Louis) was added each well of a 24-well plate and incubated at room temperature for 30 minutes. Alizarin Red solution was then removed and cells were washed four times with 1 mL water. Water (1-1.5 mL) was to cover cells in each well prior to visual inspection and image acquisition. ImageJ was used to quantify the area of red staining.¹⁹

2.7 | Rapamycin and IL-6 neutralizing antibody interference

Fibroblasts at passage 10 were cultured as described above. Cells were washed and fresh medium containing with IGFBP7 (1 µg/mL) with in water or rapamycin (500 nM, Sigma-Aldrich, Saint Louis) and 0.1% DMSO was added to cells to examine the effect of rapamycin on

IGFBP7-induced osteoblastic reprogramming P7. For the study of IL-6 signaling, IgG control antibody (50 $\mu\text{g}/\text{mL}$; Abcam, Cambridge, MA) or anti IL-6 antibody (5 $\mu\text{g}/\text{mL}$; I7901, Sigma-Aldrich, Saint Louis) was added to cells culturing in media containing IGFBP7 (1 $\mu\text{g}/\text{mL}$). Cells were grown at 37°C with 5% CO_2 , and the medium was changed every 3 days. Cells were harvested for gene expression analysis at day 4 and 14, and for Alizarin red staining at day 28.

2.8 | In vivo bone formation xenograft model

This model is adapted from Fedorovich et al.²⁰ where cultured cells are introduced into the hind limb of a nude mouse in Matrigel and bioceramic

granules. Based on prior optimization, growth factor reduced Matrigel (BD Biosciences, San Jose CA) and biphasic calcium phosphonate (BCP) microparticles 100-200 μm (Berkeley Advanced Biomaterials) were used with an optimal time of 4 weeks. Cultured human cells were harvested from tissue culture plates using trypsin, and resuspended in culture media and combined with Matrigel/BCP in a syringe with a 23-gauge needle. Two hundred microliters containing $\sim 1 \times 10^6$ cells were injected subcutaneously into the hind limbs of 8-10 week old nude (BALB/c-Fox1nu/Ausb) mice (Australian BioResources). Animals were sedated using inhaled isoflurane and given 0.1 mg/kg buprenorphine as an analgesic after the procedure. Animals were injected bilaterally.

In the first study, human fibroblasts cultured with standard and osteoblast conditioned media (OB-CM) were compared, with a no cell,

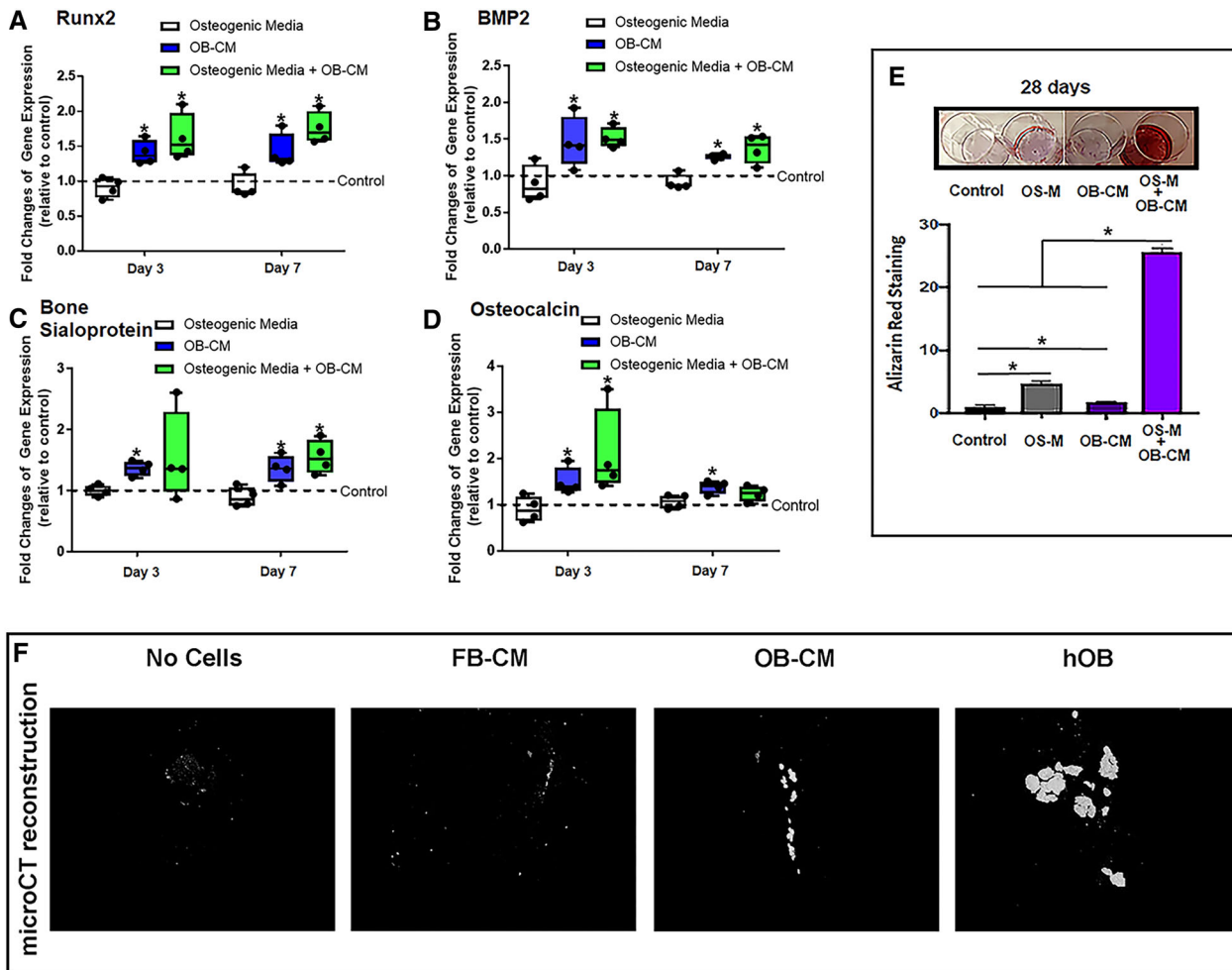


FIGURE 1 Human OB-conditioned media converts human fibroblasts into osteoblasts. Fibroblasts were treated with OB-CM, OS-M, or in combination (OB-CM+OS-M). The expression level of osteogenic markers, *Runx2*, *BMP2*, *bone sialoprotein*, and *osteocalcin*, was measured by qPCR after 3 and 7 days of culture. OB-CM or OB-CM+OS-M significantly increased expression of osteogenic genes in fibroblasts (A-D). Matrix mineralization in cells was detected by Alizarin Red S staining after 28 days of treatment. Fibroblast treated with OB-CM+OS-M exhibited greatest mineralization with an over 20-fold increase compared to control treatment (FB-CM) (E). OS-M, osteogenic components; OB-CM, osteoblast-derived conditioned media. F, Fibroblasts treated with OB-CM or FB-CM were implanted into nude mice using a carrier of Matrigel and ceramic microparticles. Mineralized tissue was analyzed by MicroCT for the total volume of mineralized bone tissue (BV). MicroCT analysis of mineralized bone (0.2 g/cm^3 threshold) showed abundant bone formation with implanted human osteoblasts, and some mineralization was observed in the mice implanted with OB-CM treated fibroblasts, but no mineralization was observed in no cell and FB-CM treated fibroblasts implantation controls. Dashed line: control (fibroblast-derived conditioned media, FB-CM). * $P \leq .05$ using ANOVA. Data were replicated in four independent experiments

and human osteoblasts as negative and positive control groups. In a second study, human fibroblasts cultured with and without the addition of IGFBP7 (1 $\mu\text{g}/\text{mL}$) were compared. Group sizes were $N = 10$ per treatment arm. Cells were cultured for 2 weeks prior to injection, and tissue from the injection site was harvested for analysis at 4 weeks post-injection.

2.9 | MicroCT and histological analysis of ectopic bone nodules

Specimens were analyzed using a Skyscan 1272 microCT scanner (Bruker, Billerica, Massachusetts) at a magnification of 5 μm , with a 0.25 mm aluminum filter, 2016 \times 1344 camera, 2050 ms exposure time, 60 kV X-ray tube voltage and 166 μA current. Scan files were reconstructed in NRecon (Bruker) using a 0.0-0.1 gray scale, and analysis was performed using CTan and BatchMan (Bruker). A volume of interest (VOI) of the tissue that encompassed the injection site was analyzed for total volume (TV) and bone volume (BV) using a cutoff for mineralized tissue of 0.3 g/cm^3 calcium calibrated to phantoms (0.25 and 0.75 g/cm^3).

All samples were harvested, fixed in 10% formalin for 24 hours and then stored in 70% ethanol. Bone nodules from the muscle pouch study were embedded in TissueTek OCT compound (Sakura, Japan) and cryosectioned to 5 μm slides using Type 2C cryofilm (Section-Lab, Hiroshima, Japan). Samples were stained for mineralized bone using previously published von Kossa staining methods.²¹

2.10 | Statistical analysis

Cell culture data were obtained from four independent experiments and represented with mean \pm SE for 5%-95% CI. A Levene's test was performed to determine the homogeneity of variance for all the data, and then an independent t test was used to analyze the data between two treatment groups. For statistical analysis involving three or more treatment groups, ANOVA was used. For ectopic bone formation studies, BV and TV values were analyzed by ANOVA with post hoc Tukey's testing to compare individual groups. For all studies, differences were considered significant if $P < .05$. Statistical analysis was performed using GraphPad Prism or SPSS 24.0.

3 | RESULTS

3.1 | Human OB-conditioned media converts human fibroblasts into osteoblasts

We hypothesized that osteoblasts produce unique combinations of factors that stimulate expression of osteoblast-specific transcripts. To test our hypothesis, we examined whether media conditioned with osteoblasts contains specific factors that trigger reprogramming of fibroblasts to express the key osteogenic markers: *Runx2* and *Osteocalcin*. Human foreskin dermal fibroblasts at passage 10 were cultured in four conditions: fibroblast-conditioned medium (FB-CM, Control), FB-CM medium supplemented with osteogenic components ascorbic acid

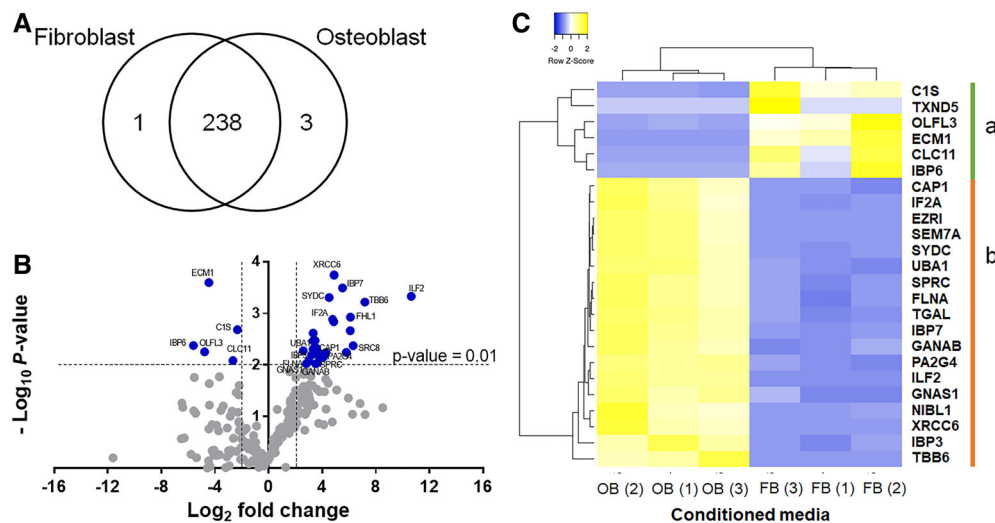


FIGURE 2 IGFBP7 is secreted by osteoblasts. Venn diagram shows the number of proteins identified in fibroblast or osteoblast conditioned medium, or in both. A total of 54 772 tandem mass spectra (MS/MS) were searched against Swissprot database using Mascot search engine with 19 138 MS/MS assigned to 1088 proteins, which was further refined to 242 human proteins (A). A volcano plot shows the identity of proteins with significant changes in their abundance (OB-CM to FB-CM). Each dot represents a protein. Thirty-five proteins with fold-change ≥ 5 and $P \leq .01$ (ANOVA) are indicated in blue dots. Proteins uniquely detected in only one medium type such as EZR1, SEM7A, and TXND5 were not shown on the plot (B). Hierarchical clustering of the 23 secreted proteins based on their standardized expression level (z-score). The proteins are clustered into two groups, clusters "a" and "b." Cluster "a" consists of proteins significantly reduced in abundance in conditioned media from osteoblast and cluster "b" consists of proteins significantly elevated in abundance in OB-CM (C). Data were replicated in two independent experiments

and β -glycerophosphate (FB-CM + AA/ β GP), osteoblast-conditioned medium (OB-CM) and OB-CM supplemented with osteogenic components (OB-CM + AA/ β GP). Fibroblasts grown in OB-CM and OB-CM + AA/ β GP (but not AA/ β GP alone) exhibited elevated expression of the osteogenic genes, *RUNX2*, *BMP2*, *bone sialoprotein*, and *osteocalcin*, after 3 and 7 days of culture (Figure 1A-D). Cells were stained with Alizarin Red S to detect matrix mineralization (extracellular calcium deposition) to assess the functional consequence of the observed osteogenic gene expression. Fibroblasts cultured in either OB-CM or AA/ β GP had two- to fivefold increase in Alizarin Red S staining compared to cells in control

media. When OB-CM + AA/ β GP were combined, however, a 20-fold increase in Alizarin Red S staining was observed (Figure 1E).

A xenograft bone formation model was used to examine the efficacy of OB-CM in modifying fibroblast phenotype in a tissue engineering setting. Cells cultured in either OB-CM or FB-CM for 14 days were implanted in the flanks of nude mice using a carrier of Matrigel and ceramic microparticles. Matrigel and ceramic microparticles carrying no cells or carrying human OB were also implanted as negative and positive controls, respectively. Mineralized tissue was analyzed by MicroCT to measure the volume of mineralized bone tissue (BV).

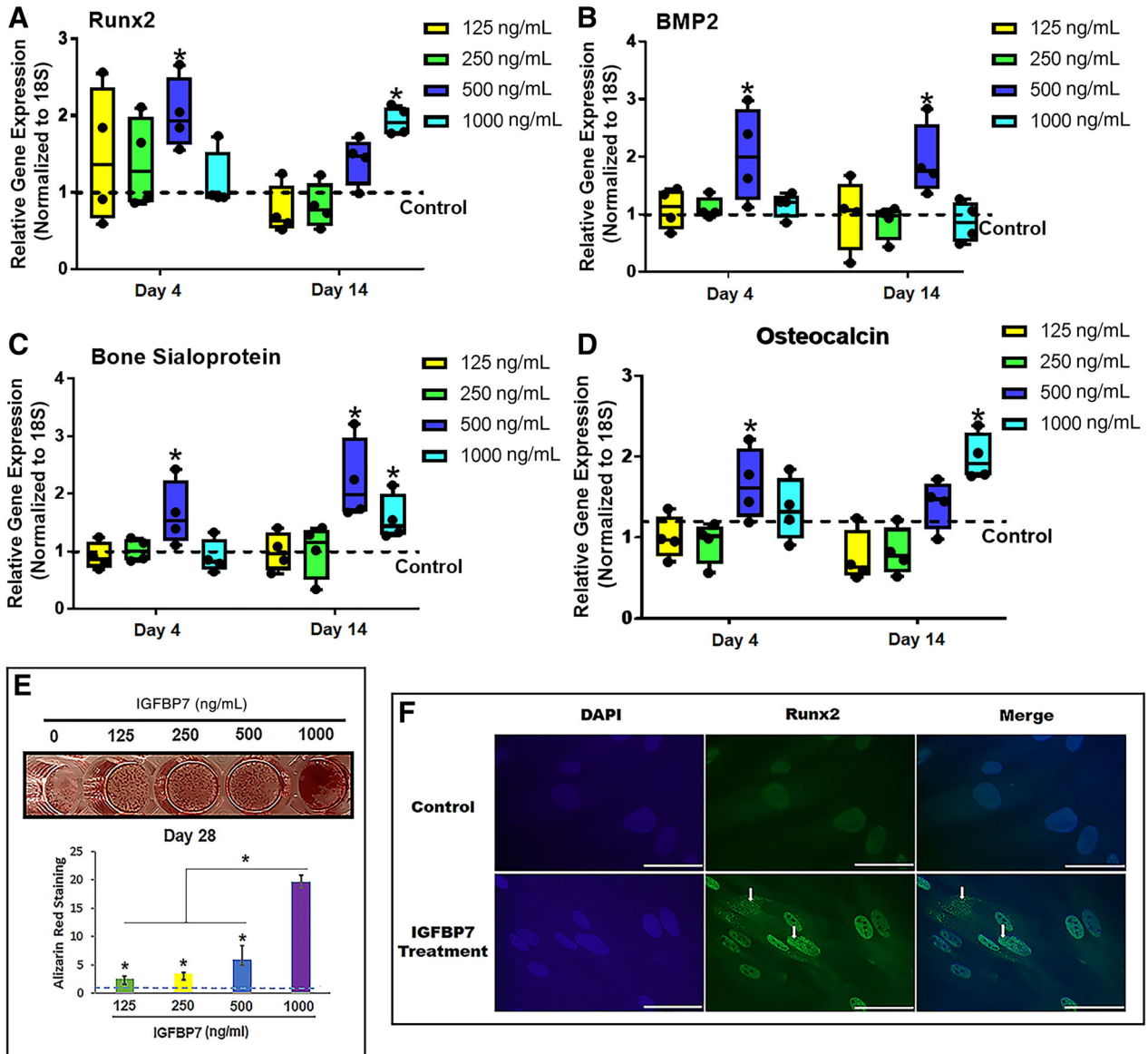


FIGURE 3 IGFBP7 reprograms fibroblasts toward an osteoblastic phenotype in vitro. Fibroblasts were cultured in growth media containing different concentrations of recombinant IGFBP7 (125–1000 ng/mL). IGFBP7 significantly increased expression of osteogenic genes (*Runx2*, *BMP2*, *bone sialoprotein*, and *osteocalcin*) in fibroblasts (A–D) at dosage of 500 and 1000 ng/mL. Matrix mineralization in cells was detected by Alizarin Red S staining after 28 days of IGFBP7 treatment. Mineralization increased in a dose-dependent manner of IGFBP7 concentration, with staining intensity >20-fold in cells treated with IGFBP7 at 1000 ng/mL (E). The proportion of fibroblasts expressing Runx2 is measured by immunostaining using anti-Runx2 antibody. Treatment of fibroblasts with 1000 ng/mL increased Runx2-positive cells from negative staining to 40% of the population (F). Dashed line: control (without IGFBP7 supplement). * $P \leq .05$ using ANOVA. Scale bar shown in panel (F) indicates 20 μ m. Data were replicated in four independent experiments

Several specimens from the OB-CM treated group showed evidence of mineralized bone in reconstructed images (Figure 1F), whereas OB-CM-treated fibroblasts did not achieve equivalent total BV levels as the positive control using human osteoblasts. Such bone nodules were not detected in animals implanted with no cells or FB-CM-treated fibroblasts.

3.2 | IGFBP7 is secreted by osteoblasts

To identify soluble factors in the secretome of osteoblasts that have the capacity to reprogram fibroblasts into functional osteoblasts, serum-free media conditioned with fibroblasts (FB-CM) or osteoblasts (OB-CM) were subjected to proteomic analysis. Principal component analysis identified that conditioned medium was the greatest variation in the experiment. Peptide ions with a $P \leq .05$ formed two distinct clusters corresponding to FB-CM or OB-CM that were 94.3% different, whereas variation between replicates was 2.5% (Supplementary Figure S1).

A total of 54 772 tandem mass spectra (MS/MS) were searched against the Swissprot database using Mascot search engine with 19 138 MS/MS assigned to 1088 proteins, which was further refined to 242 human proteins (Figure 2A). Differentially expressed proteins in OB-CM and FB-CM were identified according to their P -values and fold-change in abundance (ratio of OB-CM to FB-CM) (Figure 2B). Thirty-five proteins were found to have $P \leq .01$ and fold-change ≥ 5 (Supplementary Table S1). Of these proteins, 22 were reported to be secreted by cells based on their subcellular localization, as curated using UniProt. Transgelin, which is not annotated as secreted protein, has recently been shown to play a role in osteogenic differentiation²² and is included in the list. The 23 proteins were subjected to hierarchical clustering according to their standardized expression level (z-score) (Figure 2C) to search for potential co-regulation of protein expression. There are two major clusters: Cluster A consisted of six proteins that were significantly reduced in the OB-CM and Cluster B consisted of 18 proteins that were significantly elevated in OB-CM (Figure 2C). Two secreted proteins, EZR1 and SEM7A were uniquely observed in

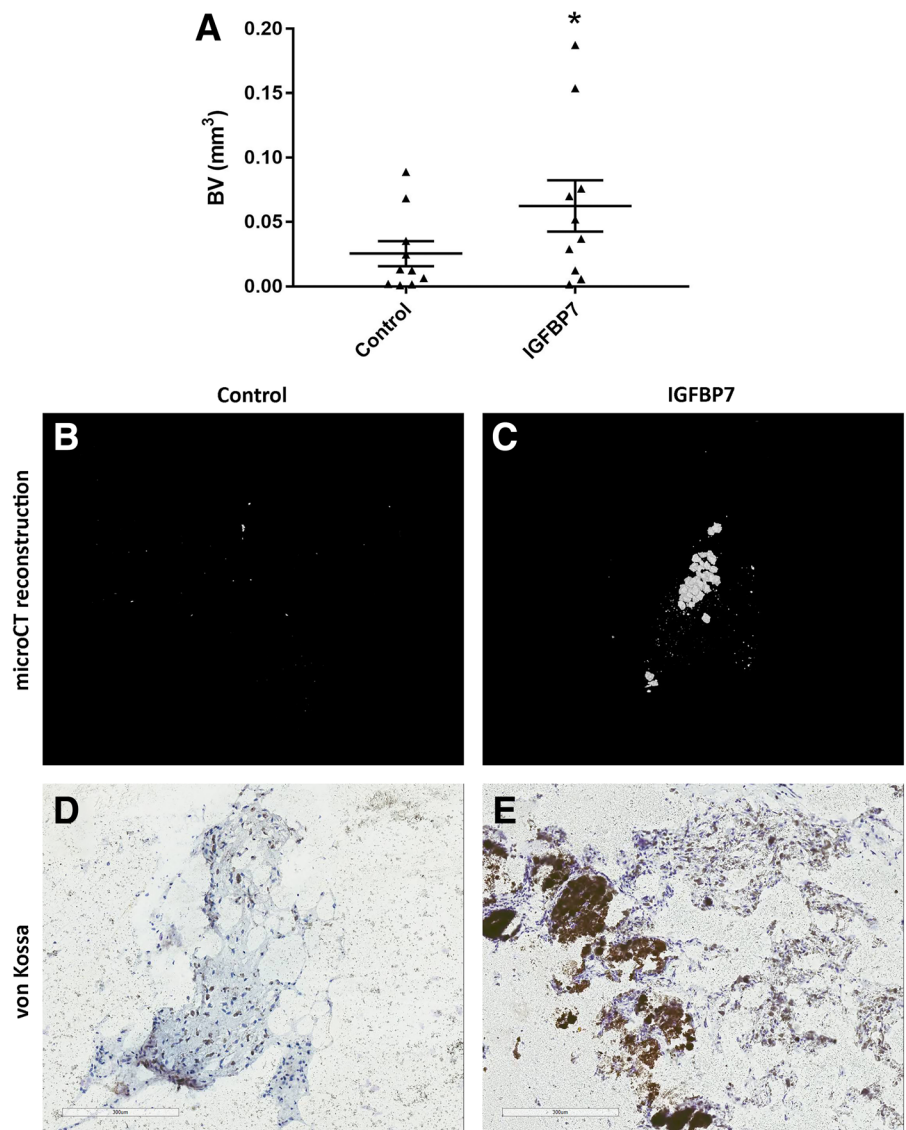


FIGURE 4 IGFBP7-treated fibroblasts form mineralized tissue in vivo. Fibroblasts treated without or with IGFBP7 (1000 ng/mL) were implanted into nude mice using a carrier of Matrigel and ceramic microparticles. Mineralized tissue was analyzed by MicroCT to measure the total volume of mineralized bone tissue (BV) and von Kossa staining for detection of mineralization in tissue. MicroCT analysis of mineralized bone (0.2 g/cm^3 threshold) showed a significant increase for IGFBP7-treated fibroblasts ($1 \mu\text{g/mL}$) $*P < .05$ vs untreated controls (A). 3D reconstructed images from MicroCT analysis are shown (B,C). Images of histological sections stained with Von Kossa are shown (D,E). Scale bars shown in (D) and (E) indicate $300 \mu\text{m}$

OB-CM while TXND5 was only identified in FB-CM. However, the abundance of these proteins was very low, accounting for only 0.2%-0.3% of the most abundant protein, FLNA.

Functional annotation analysis did not reveal enrichment of any specific biological processes (Supplementary Table S2). No overrepresentation of GO terms was found in Cluster A while Cluster B was enriched with the GO term secretion by cells (Supplementary Table S1). Among the 17 upregulated proteins in Cluster B, IBP7 (or IGFBP7) showed a 46-fold increase in abundance in OB-CM compared to FB-CM. IGFBP7 has recently been implicated in directing mesenchymal stem cells toward an osteogenic lineage.^{23,24} It has also been associated with induction of cellular senescence, which is increasingly appreciated as having a role in cellular reprogramming and tissue repair.²⁵⁻²⁹ Therefore, IGFBP7 was selected for further analysis to examine its capacity to convert fibroblasts into osteoblasts.

3.3 | IGFBP7 reprograms fibroblasts toward an osteoblastic phenotype *in vitro*

To test the ability of IGFBP7 to convert fibroblasts into osteoblasts, human foreskin fibroblasts at passage 10 were cultured in DMEM medium supplemented with increasing concentrations of IGFBP7 (0, 125, 250, 500, and 1000 ng/mL). After 4 and 14 days of culture, IGFBP7 at doses of 500 and 1000 ng/mL were able to significantly promote expression of osteogenic genes (*Runx2*, *BMP-2*, *bone sialoprotein*, and *osteocalcin*) (Figure 3A-D).

Extracellular matrix mineralization studies demonstrated that the fibroblasts treated with IGFBP7 were able to form mineralized

nodules after 28 days in a dose-dependent manner with highest response seen at 1000 ng/mL IGFBP7 (Figure 3E). Immunostaining for the osteoblast-specific lineage marker, *Runx2*, at day 14 further supports reprogramming of fibroblasts toward an osteogenic gene lineage. Approximately 40% of the cells were positive for *Runx2* (Figure 3F), while no *Runx2* positive cells were detected in untreated fibroblasts.

To further characterize the phenotype of OB induced by IGFBP7, we measured expression of embryonic stem cell maker genes (*Oct-4* and *Nanog*) and fibroblastic markers (*vimentin* and thymic stromal lymphopoietin [*TSL*]) in the IGFBP7-treated cells. IGFBP7 treatment resulted in significantly lower expression of the stem cell genes at day 4 and day 14 (Supplemental Figure S2A,B). This indicates that IGFBP7 can reprogram fibroblasts into osteoblasts without reverting to a dedifferentiated multipotent state.

3.4 | IGFBP7-treated fibroblasts form mineralized tissue *in vivo*

Prior to *in vivo* testing on the bone formation capacity of IGFBP7-treated fibroblasts 7, we treated fibroblasts with IGFBP7 (1 μ g/mL) for 4 days or 14 days to determine the optimal time-frame of IGFBP7 treatment. We found that 4 days of IGFBP7 treatment produced a reversible change of osteogenic gene expression levels in fibroblasts which dropped to basal levels seen in control group at day 14, and no significant bone nodule formation was observed at day 28 (Supplementary Figure S3A-E). In contrast, 14 days of IGFBP7 treatment on fibroblasts led to significant bone nodule formation at day 28 (Supplementary

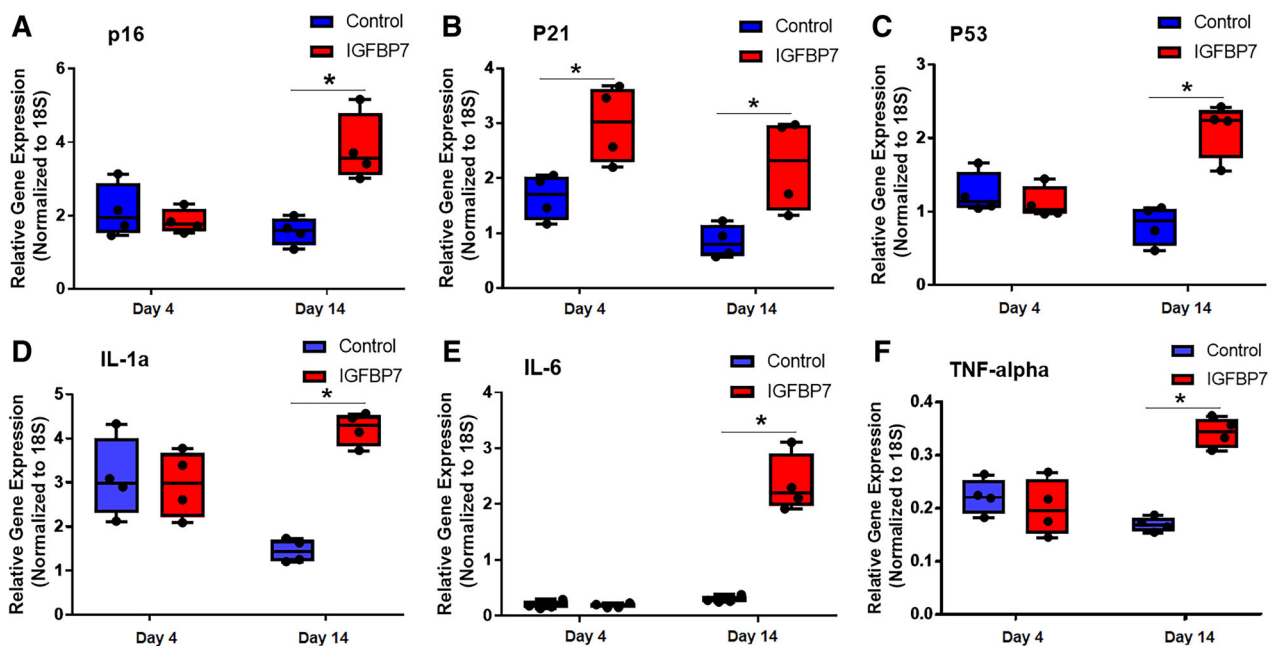


FIGURE 5 Induction of senescence plays a role in IGFBP7 reprogramming of fibroblasts to osteoblasts. Fibroblasts were treated without or with IGFBP7 (1000 ng/mL) and gene expression was measured by qPCR. IGFBP7 significantly increased expression of key senescence-associated genes (*P16*, *P21*, and *P53*; A-C) and SASP-associated genes (*IL-1 α* , *TNF- α* , and *IL-6*; D-F) at day 4 or day 14. * $P \leq .05$ when comparing to control at day 14 using a Student's *t* test. Data were replicated in four independent experiments

Figure S3E). Therefore, fibroblasts receiving 14 days of IGFBP7 treatment were used for *in vivo* study.

Fibroblasts were incubated in the absence or presence of 1 $\mu\text{g}/\text{mL}$ IGFBP7 and capacity for forming mineralized tissue was examined in a mice model same as described above. Once again, control fibroblasts showed negligible bone formation, while several specimens from the IGFBP7 treatment group showed large amounts of bone and their mean BV values were significantly higher (Figure 4). Von kossa staining confirmed the presence of mineralized tissue in the IGFBP7 treatment group and nodules were observed in reconstructed images from microCT analysis.

3.5 | Induction of senescence plays a role in IGFBP7 reprogramming of fibroblasts to osteoblasts

Increasing evidence indicates that cell senescence plays a key role in regulating cellular plasticity in tissue repair and regeneration.²⁹⁻³¹ We examined IGFBP7-induced cell senescence in the fibroblast to osteoblast transition. IGFBP7 significantly increased expression of key gene regulators of cell senescence such as *P16*, *P21*, and *P53* at day 4 and day 14 of culture (Figure 5A-C). Additionally, we also measured the gene expression levels of *IL- α* , *TNF- α* , and *IL-6*, which are among a plethora of proteins collectively termed senescence associated secretory profiles (SASP) secreted by

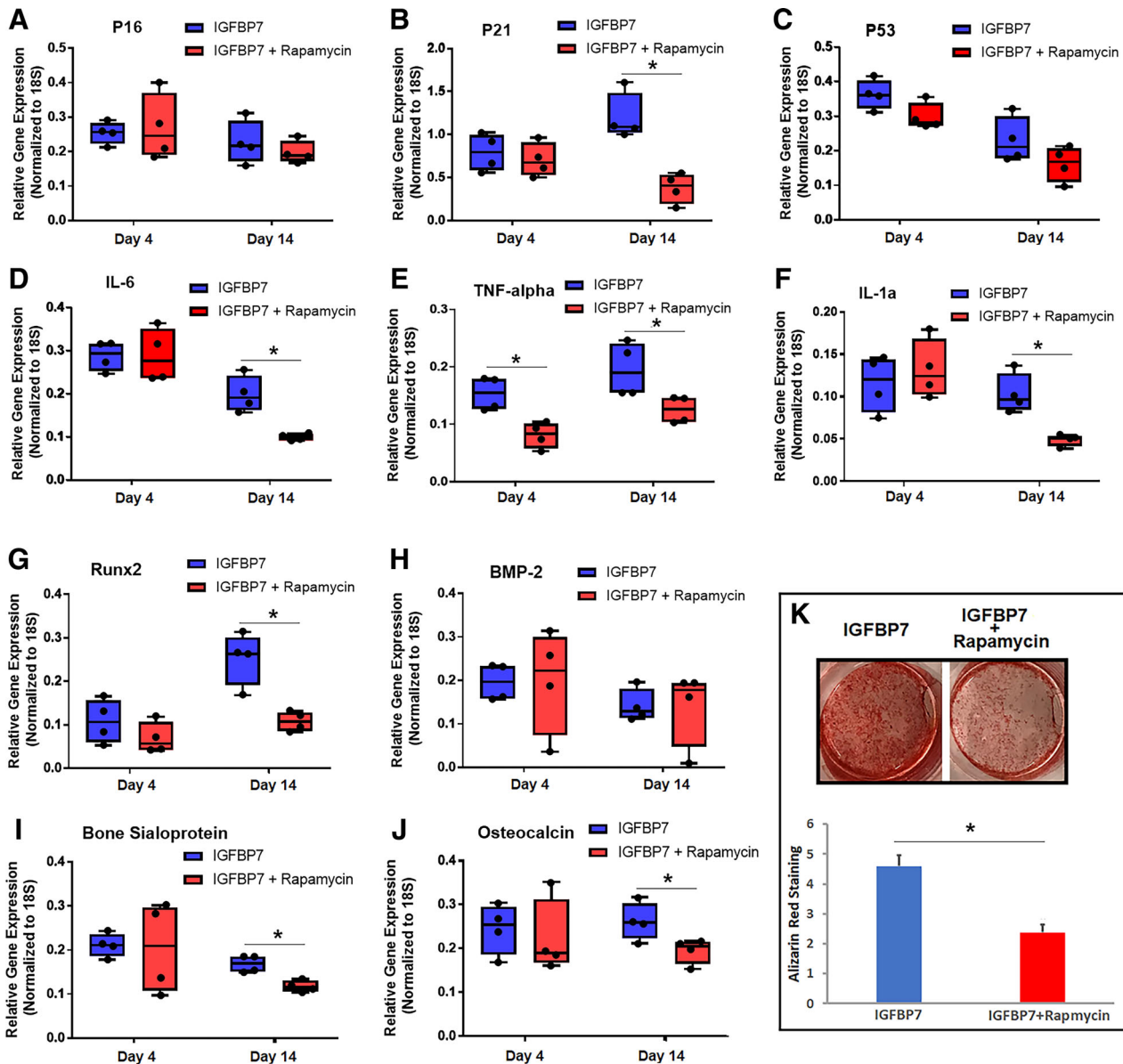


FIGURE 6 The senescence inhibitor, rapamycin, antagonizes IGFBP7 reprogramming in fibroblast. Fibroblasts were treated with IGFBP7 (1000 ng/mL) alone or in combination with rapamycin (500 μM) and gene expression was measured by qPCR. Rapamycin decreased expression of senescence-associated genes (*P16*, *P21*, and *P53*; A-C), SASP-associated genes (*IL-1 α* , *TNF- α* , and *IL-6*; D-F) and osteogenic genes (*Runx2*, *BMP-2*, *bone sialoprotein*, and *osteocalcin*; G-J). Matrix mineralization and bone nodules formation were also impaired in cells treated with rapamycin (K). * $P < .05$ when comparing to IGFBP7 treatment only at day 14 using a Student's *t* test. Data were replicated in four independent experiments

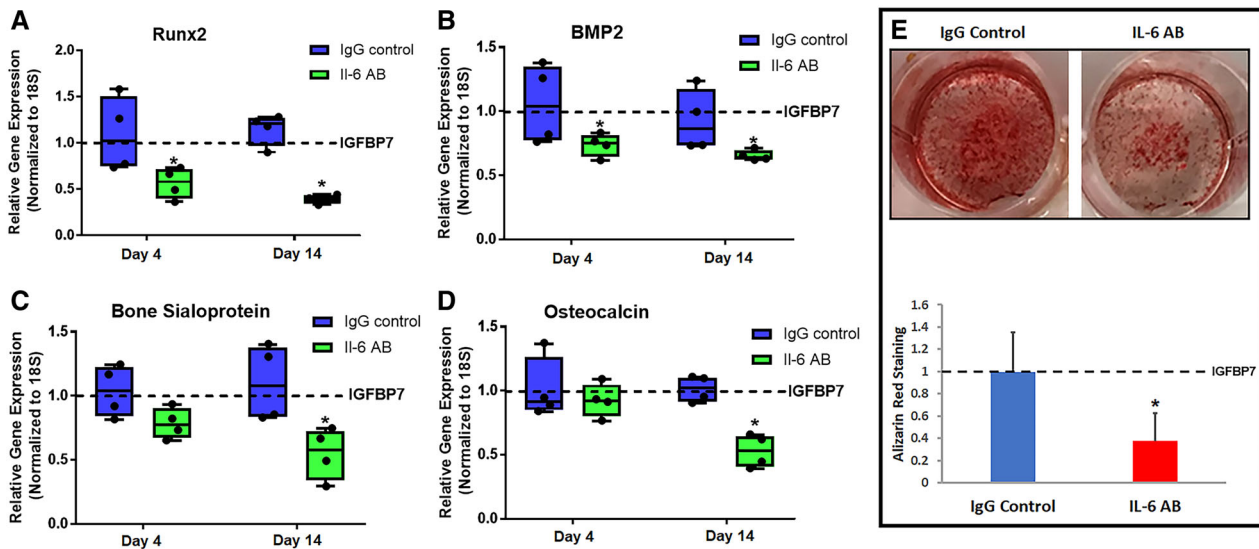


FIGURE 7 IGFBP7-induced osteoblastic reprogramming is dependent on IL-6. Fibroblasts were treated with IGFBP7 (1000 ng/mL) together with IgG control antibody (50 μ g/mL) or IL-6 neutralizing antibody (5 μ g/mL). Expression of osteogenic genes (*Runx2*, *BMP-2*, *bone sialoprotein*, and *osteocalcin*) were measured by qPCR. Addition of IL-6 neutralizing antibody significantly reduced osteogenic gene expression (A-D), and decrease in matrix mineralization and nodules formed (E). * $P \leq .05$ when comparing to IgG control antibody 14 using ANOVA. Data were replicated in four independent experiments

metabolically active senescent cells, and found that they were also significantly elevated by IGFBP7 treatment (Figure 5D-F). Notably, cells were negative for senescence-associated beta-galactosidase (SA- β -gal) staining after 14 and 21 days of culture.

To further investigate if senescence induction plays a role in IGFBP7 reprogramming of fibroblasts to osteoblasts, the cell senescence inhibitor, rapamycin,^{32,33} was employed. Rapamycin reduced expression of cell senescence regulator genes (*P16*, *P21*, and *P53*) and SASP expression (*IL- α* , *TNF- α* , and *IL-6*) (Figure 6A-F). Moreover, rapamycin inhibited trans-differentiation of fibroblasts by decreasing the expression of osteogenic genes (*Runx2*, *BMP-2*, *bone sialoprotein*, and *osteocalcin*, Figure 6G-J) and thus diminished the formation of mineralized nodules (Figure 6K).

Contribution of IGF signaling pathway in fibroblast reprogramming was assessed by comparing IGFBP1 with IGFBP7 in trans-differentiation, as IGFBP1 has a 100-fold increased affinity for IGF.³⁴ But IGFBP1 treatment did not change expression of osteoblastic gene markers, or expression of senescence-associated regulatory genes (*P16*, *P21*, and *P53*) and SASP genes (*IL-6*) (Supplementary Figure S4A-H). This suggests that osteoblastic reprogramming by IGFBP7 is independent of canonical IGF signaling.

3.6 | IGFBP7-induced osteoblastic reprogramming is dependent on IL-6

Of the SASP factors, expression of IL-6 was the highest in the cells after 14 days of culture with IGFBP7 (~10-fold). To investigate the dependence of IGFBP7-mediated osteoblastic reprogramming on autocrine action of IL-6, secreted IL-6 was neutralized with a blocking

antibody. Inhibiting IL-6 significantly reduced expression of several osteogenic genes (*Runx2*, *BMP-2*, *bone sialoprotein*, and *osteocalcin*, Figure 7A-D) in the fibroblasts and formation of mineralized nodules by Alizarin red staining (Figure 7E). This suggests that IGFBP7 triggers an IL-6 dependent pathway in the osteoblastic reprogramming of fibroblasts.

4 | DISCUSSION

Tissue engineering is a growing field of research focusing on regeneration of damaged tissues with minimal scar formation. Regeneration strategies commonly employ cell-seeded constructs that enable cells to functionally assume the phenotype of the target tissue. In comparison to other commonly used cell sources, the use of skin fibroblasts for tissue regeneration has significant advantages. For instance, they overcome the drawbacks of iPSCs, including complex production processes and risk of teratoma formation, and will require a much less invasive collection procedure and deliver a much higher yield than adult mesenchymal stem cells; in addition, adult mesenchymal stem cells lose their capacity for differentiation after 5 passages in vitro,³⁵ while adult skin fibroblasts can undergo 15 passages. However, since fibroblasts are differentiated cells, it is challenging to redirect fibroblast toward specific lineages. We report herein that the protein, IGFBP7, identified from the secretome of osteoblasts, can reprogram human fibroblasts into OB, and IGFBP7 induces a senescent phenotype and autocrine IL-6 signaling during the reprogramming.

Genetic approaches have successfully converted dermal fibroblasts into osteoblasts in several studies.³⁶⁻³⁹ For example, over-expression of the muscle master transcription factor *MyoD* in

myoblasts can increase their sensitivity to bone morphogenetic protein (BMP-2), thus enhancing BMP signaling to drive trans-differentiation into OB. Fibroblasts, however, are normally insensitive to BMP-2 suggesting that other factors are necessary to induce conversion to osteoblasts.⁴⁰ The progress with lineage conversion by genetic manipulation is promising, however it offers little control for maintaining cell lineage over time. In addition, viral constructs that are commonly employed in gene transfection also pose safety concerns for clinical use. In contrast, exogenous factors that can modify lineage specificity have greater immediate potential for translation in comparison to gene modification technologies. For example, a kinase inhibitor (ALK5 inhibitor II) that inhibits transforming growth factor β (TGF- β) signaling, which is central to fibrogenesis,⁴¹ was used in one study to reprogram fibroblasts into osteoblast cells,³⁹ although kinase inhibitors, that target a range of alternative targets, may lead to severe toxicity thus rendering their unsuitability usage in tissue engineering.

Using a proteomics approach we identified a number of candidate factors that are differentially expressed in the secretome of osteoblasts compared to that of fibroblasts. Among them, IGFBP7 is the most promising candidate based on recent reports on its involvement in bone diseases and osteogenic differentiation in mesenchymal stem cells.^{23,24} Our *in vitro* and *in vivo* studies support IGFBP7 as potent protein for osteoblastic reprogramming of fibroblasts. We firstly showed that IGFBP7 upregulates expression of osteoblastic markers in cultured fibroblast cells. Then an *in vitro* study was performed to investigate if a bone inductive protein, BMP2, has a similar osteogenic reprogramming efficacy with IGFBP7. The results showed that BMP2 (100 ng/mL) did not significantly elevate osteogenic gene expression levels in the fibroblasts (Supplementary Figure S5) after 14 days of treatment, suggesting that IGFBP7 is a novel and potent protein for osteoblastic reprogramming of fibroblasts. In addition, we observed that 4 days of IGFBP7 treatment produced a reversible change in osteogenic gene expression in fibroblasts, indicating that a short-term (eg, 4 days) IGFBP7 exposure only leads to a reversible alteration of cellular epigenetic states in fibroblasts. More studies would be needed to examine at what point osteogenic trans-differentiation becomes irreversible following IGFBP7 treatment *in vitro* and *in vivo*.

The *in vivo* xenograft system is a stringent model for testing osteoblastic activity since it does not produce mineralized tissue when using non-bone cell types nor when alternative bioceramic microparticles are employed.²⁰ Using this model, we observed no significant bone formation using fibroblast cells treated with OB-CM, whereas treatment with 1 μ g/mL of recombinant IGFBP7 resulted in statistically significant increase in BV. Although the implanted IGFBP7-treated fibroblasts did not give rise to the same amount of bone nodule formation in comparison to that of human osteoblasts, further optimization of bone formation by modulating IGFBP7 concentrations, duration and cofactors may improve bone nodule formation. It may be possible to produce high quality functional OB from fibroblasts for therapeutic application by incorporating known pro-osteogenic factors for differentiation in a two-step approach; where fibroblasts are first sensitized with IGFBP7 followed by treatment using pro-osteogenic supplements and bioactive proteins.

Our findings also provide insights the mechanism of IGFBP7-mediated reprogramming in fibroblasts. IGFBP7 belongs to the IGF binding protein family. Unlike IGFBP1-6, which all bind insulin-like growth factor (IGF) with high affinity, IGFBP7 lacks the C terminus and has a 100-fold reduced affinity for IGF.³⁴ IGF binding function is not important for IGFBP7 osteoblastic reprogramming, as high affinity IGF binder, IGFBP1, does not induce expression of osteoblastic markers or senescent phenotype in fibroblasts.

Cell senescence is a form of cell cycle arrest characterized by the activation of tumor suppressor networks including p53, p16, and p21, and production of SASP factors. Cellular senescence is regarded as detrimental for tissue repair and regeneration since it induces replicative aging in cells,⁴² which directly contributes to their loss of regenerative capacity in tissue repair.⁴³⁻⁴⁶ Additionally, SASP proteins released by senescent cells can disrupt tissue homeostasis and potentially act on neighboring cells in a paracrine signaling manner.^{45,47-49} Thus, induction of cell senescence in the reprogramming of fibroblast into OB appears contradictory. Nevertheless, emerging evidence in embryonic and adult tissues indicates that cell senescence is beneficial in tissue homeostasis.^{28,29,31,50,51} Indeed, we found that induction of cell senescence is required for trans-differentiation. Rapamycin, which is a well-established inhibitor for cell senescence,^{32,33,52} antagonized the induction of senescence in fibroblasts by IGFBP7 and abolished reprogramming into osteoblasts. It is possible that activation of other signaling pathways by IGFBP7 also contributes to osteogenic phenotype in fibroblasts. For instance, it has been shown that IGFBP7 can activate Wnt signaling that is important for upregulation of osteogenic gene expression and bone repair.^{23,24}

It is notable that that we did not detect positive staining for SA- β -gal in IGFBP7-treated cells, indicating IGFBP7 does not induce fibroblasts into the end stage of cellular senescence characterized with irreversible and permanent cell-cycle arrest, and more likely into a transient cell-cycle arrest. We speculate that such a transient cell-cycle arrest might share some common properties with cell senescence such as cell-cycle arrest and production of SASP molecules. In order to gain more insight into the role of senescence in cellular reprogramming, we carried out another study investigating if IGFBP7 is able to reprogram aged fibroblasts at passage 20 into osteoblastic lineage, as repeated passaging induces a replicative senescence phenotype with permanent cell-cycle arrest.⁵³ We showed that aged fibroblasts (passage 20) did not response to IGFBP7 treatment with no elevated osteogenic gene expression levels (Supplementary Figure S6). Such a result reinforced our speculation that IGFBP7 might only induce fibroblasts into a transient cell-cycle arrest, although the underlying mechanism remains unclear. Another finding of this study is that the expression of the SASP protein, IL-6, which is also a pro-inflammatory cytokine, was markedly upregulated in IGFBP7-treated fibroblasts. Importantly, IL-6 and its receptor, IL-6R, are elevated in bone-derived mesenchymal stem cells, and IL-6 signaling activates STAT3 phosphorylation and downstream signaling to induce osteogenic gene expression.^{54,55} Our study showed that neutralization of secreted IL-6 abrogated fibroblast to osteoblast reprogramming, suggesting a key role of autocrine IL-6 signaling in IGFBP-mediated

osteoblastic reprogramming. However, other mechanisms might also be worthy of investigation. For instance, it was reported that IGFBP7 induces cellular senescence in young mesenchymal stem cells via a reversal DNA-damage response.²⁵

One limitation of our study was the use of conventional bone markers to measure osteoblastic reprogramming. Our approach provides snapshots rather than a complete overview of the transcriptomic profile during reprogramming. Future studies employing RNA sequencing at single cell level could provide a better understanding of transcriptomic and epigenetic changes in trans-differentiated cells. However, our findings identify IGFBP7 as an important exogenous factor that can convert fibroblasts to functional osteoblasts.

Future analyses of the functions of other proteins identified in osteoblast conditioned media, and their ability to augment the pro-osteogenic activity of IGFBP7, will advance our understanding of osteogenic differentiation in fibroblasts. Optimization of ex vivo trans-differentiation of fibroblasts into osteoblasts will pave the way to use fibroblasts as a source for osteoblasts for regenerating bone with application to more sophisticated orthopedic tissue engineering models in the future.

ACKNOWLEDGMENTS

We are grateful for financial support from the National Health and Medical Research Council (NHMRC) Early Career Fellowships (APP1036370) and the University of Sydney Bridging Fellowship; Australian Research Council (H.Z. and C.R.D.), National Health and Medical Research Council of Australia (APP1110219 to P.J.H.) and (APP1139515 to H.Z., C.R.D., and A.S.); and Helen and Robert Ellis Postdoctoral Fellowship and Tony Basten Postdoctoral Fellowship from the Sydney Medical School Foundation to J.C. L.R.L. is the recipient of an Australian Government Research Training Program (RTF) scholarship.

CONFLICT OF INTEREST

C.D. declared advisory role and the license of intellectual property to Allegra Orthopaedics for a bioceramic material; stock ownership of Cochlear, CSL, and ResMed shares. The other authors indicated no potential conflicts of interest.

AUTHOR CONTRIBUTIONS

Z.L.: conception and design, financial support, collection and/or assembly of data, data analysis and interpretation, manuscript writing, final approval of manuscript; J.C.: collection and/or assembly of data, data analysis and interpretation, manuscript writing, final approval of manuscript; P.J.H.: financial support, data analysis and interpretation, manuscript writing, final approval of manuscript; L.L., M.J., Y.R., C.D.: collection and/or assembly of data, final approval of manuscript; A.S.: collection and/or assembly of data, data analysis and interpretation, final approval of manuscript; H.Z.: conception and design, financial support, data analysis and interpretation, manuscript writing, final approval of manuscript.

DATA AVAILABILITY STATEMENT

The data that support the findings of this study are available from the corresponding author upon reasonable request.

ORCID

ZuFu Lu  <https://orcid.org/0000-0003-4843-4441>

REFERENCES

1. Assou S, Bouckenheimer J, De Vos J. Concise Review: assessing the genome integrity of human induced pluripotent stem cells: what quality control metrics? *STEM CELLS*. 2018;36:814-821.
2. Avaliani N, Pfisterer U, Heuer A, Parmar M, Kokaia M, Andersson M. Directly converted human fibroblasts mature to neurons and show long-term survival in adult rodent hippocampus. *Stem Cells Int*. 2017;2017:1-9.
3. Fu Y, Huang C, Xu X, et al. Direct reprogramming of mouse fibroblasts into cardiomyocytes with chemical cocktails. *Cell Res*. 2015;25:1013-1024.
4. Simeonov KP, Uppal H. Direct reprogramming of human fibroblasts to hepatocyte-like cells by synthetic modified mRNAs. *PLoS One*. 2014;9:e100134.
5. Sinha M, Sen CK, Singh K, et al. Direct conversion of injury-site myeloid cells to fibroblast-like cells of granulation tissue. *Nat Commun*. 2018;9:936.
6. Yang Y, Li Z, Wu X, et al. Direct reprogramming of mouse fibroblasts toward leydig-like cells by defined factors. *Stem Cell Rep*. 2017;8:39-53.
7. Okita K, Ichisaka T, Yamanaka S. Generation of germline-competent induced pluripotent stem cells. *Nature*. 2007;448:313-317.
8. Li W, Sun W, Zhang Y, et al. Rapid induction and long-term self-renewal of primitive neural precursors from human embryonic stem cells by small molecule inhibitors. *Proc Natl Acad Sci USA*. 2011;108:8299-8304.
9. Li W, Jiang K, Ding S. Concise review: a chemical approach to control cell fate and function. *STEM CELLS*. 2012;30:61-68.
10. Zhang Y, Li W, Laurent T, Ding S. Small molecules, big roles – the chemical manipulation of stem cell fate and somatic cell reprogramming. *J Cell Sci*. 2012;125:5609-5620.
11. Zhu S, Li W, Zhou H, et al. Reprogramming of human primary somatic cells by OCT4 and chemical compounds. *Cell Stem Cell*. 2010;7:651-655.
12. Ducy P, Zhang R, Geoffroy V, Ridall AL, Karsenty G. *Osf2/Cbfa1*: a transcriptional activator of osteoblast differentiation. *Cell*. 1997;89:747-754.
13. Ducy P, Schinke T, Karsenty G. The osteoblast: a sophisticated fibroblast under central surveillance. *Science*. 2000;289:1501-1504.
14. Lu Z, Roohani-Esfahani SI, Wang G, Zreiqat H. Bone biomimetic microenvironment induces osteogenic differentiation of adipose tissue-derived mesenchymal stem cells. *Nanomedicine*. 2012;8:507-515.
15. Kulasingam V, Diamandis EP. Proteomics analysis of conditioned media from three breast cancer cell lines: a mine for biomarkers and therapeutic targets. *Mol Cell Proteomics*. 2007;6:1997-2011.
16. Qi D, Brownridge P, Xia D, et al. A software toolkit and interface for performing stable isotope labeling and top3 quantification using Progenesis LC-MS. *Omics*. 2012;16:489-495.
17. Babicki S, Arndt D, Marcu A, et al. Heatmapper: web-enabled heat mapping for all. *Nucleic Acids Res*. 2016;44:W147-W153.
18. Mi H, Huang X, Muruganujan A, et al. PANTHER version 11: expanded annotation data from Gene Ontology and Reactome pathways, and data analysis tool enhancements. *Nucleic Acids Res*. 2017;45:D183-D189.
19. Lu Z, Chen Y, Dunstan C, Roohani-Esfahani S, Zreiqat H. Priming adipose stem cells with tumor necrosis factor- α preconditioning potentiates their exosome efficacy for bone regeneration. *Tissue Eng Part A*. 2017;23:1212-1220.
20. Fedorovich NE, Leeuwenburgh SC, van der Helm YJ, Alblas J, Dhert WJ. The osteoinductive potential of printable, cell-laden

- hydrogel-ceramic composites. *J Biomed Mater Res A*. 2012;100:2412-2420.
21. McDonald MM, Morse A, Birke O, et al. Sclerostin antibody enhances bone formation in a rat model of distraction osteogenesis. *J Orthop Res*. 2018;36:1106-1113.
 22. Elsafadi M, Manikandan M, Dawud RA, et al. Transgelin is a TGF beta-inducible gene that regulates osteoblastic and adipogenic differentiation of human skeletal stem cells through actin cytoskeleton organization. *Cell Death Dis*. 2016;7:e2321.
 23. Zhang W, Chen E, Chen M, et al. IGFBP7 regulates the osteogenic differentiation of bone marrow-derived mesenchymal stem cells via Wnt/beta-catenin signaling pathway. *FASEB J*. 2018;32:2280-2291.
 24. Infante A, Rodriguez CI. Secretome analysis of in vitro aged human mesenchymal stem cells reveals IGFBP7 as a putative factor for promoting osteogenesis. *Sci Rep*. 2018;8:4632.
 25. Severino V, Alessio N, Farina A, et al. Insulin-like growth factor binding proteins 4 and 7 released by senescent cells promote premature senescence in mesenchymal stem cells. *Cell Death Dis*. 2013;4:e911.
 26. Wajapeyee N, Serra RW, Zhu X, Mahalingam M, Green MR. Role for IGFBP7 in senescence induction by BRAF. *Cell*. 2010;141:746-747.
 27. Chiche A, Le Roux I, von Joest M, et al. Injury-induced senescence enables in vivo reprogramming in skeletal muscle. *Cell Stem Cell*. 2017;20:407-414.e404.
 28. Mosteiro L, Pantoja C, Alcazar N, et al. Tissue damage and senescence provide critical signals for cellular reprogramming in vivo. *Science*. 2016;354:aaf4445.
 29. Ritschka B, Storer M, Mas A, et al. The senescence-associated secretory phenotype induces cellular plasticity and tissue regeneration. *Genes Dev*. 2017;31:172-183.
 30. Farr JN, Khosla S. Cellular senescence in bone. *Bone*. 2019;121:121-133.
 31. Demaria M, Ohtani N, Youssef SA, et al. An essential role for senescent cells in optimal wound healing through secretion of PDGF-AA. *Dev Cell*. 2014;31:722-733.
 32. Shuai Y, Liao L, Su X, et al. Melatonin treatment improves mesenchymal stem cells therapy by preserving stemness during long-term in vitro expansion. *Theranostics*. 2016;6:1899-1917.
 33. Zhao P, Sui BD, Liu N, et al. Anti-aging pharmacology in cutaneous wound healing: effects of metformin, resveratrol, and rapamycin by local application. *Aging Cell*. 2017;16:1083-1093.
 34. Yamanaka Y, Wilson EM, Rosenfeld RG, Oh Y. Inhibition of insulin receptor activation by insulin-like growth factor binding proteins. *J Biol Chem*. 1997;272:30729-30734.
 35. Oliveira PH, Boura JS, Abecasis MM, Gimble JM, da Silva CL, Cabral JMS. Impact of hypoxia and long-term cultivation on the genomic stability and mitochondrial performance of ex vivo expanded human stem/stromal cells. *Stem Cell Res*. 2012;9:225-236.
 36. Mizoshiri N, Kishida T, Yamamoto K, et al. Transduction of Oct6 or Oct9 gene concomitant with Myc family gene induced osteoblast-like phenotypic conversion in normal human fibroblasts. *Biochem Biophys Res Commun*. 2015;467:1110-1116.
 37. Yamamoto K, Kishida T, Sato Y, et al. Direct conversion of human fibroblasts into functional osteoblasts by defined factors. *Proc Natl Acad Sci USA*. 2015;112:6152-6157.
 38. Yamamoto K, Sato Y, Honjo K, et al. Generation of directly converted human osteoblasts that are free of exogenous gene and xenogenic protein. *J Cell Biochem*. 2016;117:2538-2545.
 39. Yamamoto K, Kishida T, Nakai K, et al. Direct phenotypic conversion of human fibroblasts into functional osteoblasts triggered by a blockade of the transforming growth factor-beta signal. *Sci Rep*. 2018;8:8463.
 40. Liu R, Ginn SL, Lek M, et al. Myoblast sensitivity and fibroblast insensitivity to osteogenic conversion by BMP-2 correlates with the expression of Bmpr-1a. *BMC Musculoskelet Disord*. 2009;10:51.
 41. Biernacka A, Dobaczewski M, Frangogiannis NG. TGF-beta signaling in fibrosis. *Growth Factors*. 2011;29:196-202.
 42. Dimri GP, Lee X, Basile G, et al. A biomarker that identifies senescent human cells in culture and in aging skin in vivo. *Proc Natl Acad Sci USA*. 1995;92:9363-9367.
 43. Nishiguchi MA, Spencer CA, Leung DH, Leung TH. Aging suppresses skin-derived circulating SDF1 to promote full-thickness tissue regeneration. *Cell Rep*. 2018;25:3898.
 44. Orioli D, Dellambra E. Epigenetic regulation of skin cells in natural aging and premature aging diseases. *Cell*. 2018;7:e268.
 45. Sahu A, Mamiya H, Shinde SN, et al. Age-related declines in alpha-Klotho drive progenitor cell mitochondrial dysfunction and impaired muscle regeneration. *Nat Commun*. 2018;9:4859.
 46. Khong SML, Lee M, Kosaric N, et al. Single-cell transcriptomics of human mesenchymal stem cells reveal age-related cellular subpopulation depletion and impaired regenerative function. *STEM CELLS*. 2019;37:240-246.
 47. Hiebert P, Wietecha MS, Cangkrama M, et al. Nrf2-mediated fibroblast reprogramming drives cellular senescence by targeting the matrisome. *Dev Cell*. 2018;46:145-161.e110.
 48. Jeon OH, Kim C, Laberge RM, et al. Local clearance of senescent cells attenuates the development of post-traumatic osteoarthritis and creates a pro-regenerative environment. *Nat Med*. 2017;23:775-781.
 49. Varela-Eirin M, Varela-Vazquez A, Guitian-Caamano A, et al. Targeting of chondrocyte plasticity via connexin43 modulation attenuates cellular senescence and fosters a pro-regenerative environment in osteoarthritis. *Cell Death Dis*. 2018;9:1166.
 50. Munoz-Espin D, Canamero M, Maraver A, et al. Programmed cell senescence during mammalian embryonic development. *Cell*. 2013;155:1104-1118.
 51. Storer M, Mas A, Robert-Moreno A, et al. Senescence is a developmental mechanism that contributes to embryonic growth and patterning. *Cell*. 2013;155:1119-1130.
 52. Haller S, Kapuria S, Riley RR, et al. mTORC1 activation during repeated regeneration impairs somatic stem cell maintenance. *Cell Stem Cell*. 2017;21:806-818 e805.
 53. Wagner W, Horn P, Castoldi M, et al. Replicative senescence of mesenchymal stem cells: a continuous and organized process. *PLoS One*. 2008;3:e2213.
 54. Xie Z, Tang S, Ye G, et al. Interleukin-6/interleukin-6 receptor complex promotes osteogenic differentiation of bone marrow-derived mesenchymal stem cells. *Stem Cell Res Ther*. 2018;9:13.
 55. Huang RL, Sun Y, Ho CK, et al. IL-6 potentiates BMP-2-induced osteogenesis and adipogenesis via two different BMPR1A-mediated pathways. *Cell Death Dis*. 2018;9:144.

SUPPORTING INFORMATION

Additional supporting information may be found online in the Supporting Information section.

How to cite this article: Lu ZF, Chiu J, Lee LR, et al. Reprogramming of human fibroblasts into osteoblasts by insulin-like growth factor-binding protein 7. *STEM CELLS Transl Med*. 2020;9:403-415. <https://doi.org/10.1002/sctm.19-0281>